

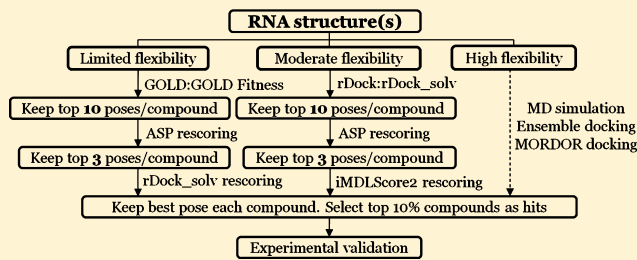
Novel Insights of Structure-Based Modeling for RNA-Targeted Drug Discovery

Lu Chen,[†] George A. Calin,^{†,‡} and Shuxing Zhang^{*,†}

[†]Integrated Molecular Discovery Laboratory, Department of Experimental Therapeutics, and [‡]The Center for RNA Interference and Non-Coding RNAs, The University of Texas M.D. Anderson Cancer Center, 1901 East Road, Houston Texas 77054, United States

 Supporting Information

ABSTRACT: Substantial progress in RNA biology highlights the importance of RNAs (e.g., microRNAs) in diseases and the potential of targeting RNAs for drug discovery. However, the lack of RNA-specific modeling techniques demands the development of new tools for RNA-targeted rational drug design. Herein, we implemented integrated approaches of accurate RNA modeling and virtual screening for RNA inhibitor discovery with the most comprehensive evaluation to date of five docking and 11 scoring methods. For the first time, statistical analysis was heavily employed to assess the significance of our predictions. We found that GOLD:GOLD Fitness and rDock:rDock_solv could accurately predict the RNA ligand poses, and ASP rescoring further improved the ranking of ligand binding poses. Due to the weak correlations ($R^2 < 0.3$) of existing scoring with experimental binding affinities, we implemented two new RNA-specific scoring functions, iMDLScore1 and iMDLScore2, and obtained better correlations with $R^2 = 0.70$ and 0.79, respectively. We also proposed a multistep virtual screening approach and demonstrated that rDock:rDock_solv together with iMDLScore2 rescoring obtained the best enrichment on the flexible RNA targets, whereas GOLD:GOLD Fitness combined with rDock_solv rescoring outperformed other methods for rigid RNAs. This study provided practical strategies for RNA modeling and offered new insights into RNA–small molecule interactions for drug discovery.



INTRODUCTION

The recent substantial progress in RNA biology underscores the importance of RNA in normal and aberrant cellular functions. It also highlights the potential of targeting RNA for treatment of a multitude of diseases including bacterial/viral infection^{1,2} and cancer.^{3,4} RNAs can form well-defined tertiary structures, such as double helices, hairpins, bulges, and pseudoknots, which offer structural bases for designing therapeutic agents. As a matter of fact, some structured RNAs, including bacterial 16S rRNAs (rRNA), HIV-1 TAR RNAs, and small non-coding microRNAs (miRNAs), exhibit attractive structural and functional characteristics similar to those of proteins.⁵ We have linked miRNAs to different diseases including cancer,^{6,7} and recently embarked on the discovery of small molecule inhibitors targeting miRNAs (SMIR).^{8,9} Druggable RNA targets are largely unexplored,¹⁰ and RNA inhibitors, such as aminoglycosides which are for the most well-defined RNA target—16S rRNA A-site—usually have poor selectivity or oral bioavailability. There have been several reports in targeting the prokaryotic rRNA A-site,^{11–13} HIV-1 TAR RNA,^{14–16} and riboswitches^{17–19} with small molecules. Researchers are also exploring new generations of druglike molecules targeting pathogenic or human disease-related RNAs including CUG- or CCUG-repeated mRNA,^{20–22} miRNA,^{23,24} and internal ribosome entry site (IRES).^{25,26} These studies provided proofs of the principle that RNAs can

be specifically targeted for antiviral or anticancer therapeutic development.

Structure-based modeling techniques, such as molecular docking, have been widely used in the field of protein-targeted drug discovery; however, most of these *in silico* methodologies were developed for proteins. Mature tools specific for RNAs (e.g., virtual screening for RNA inhibitor identification) are lacking.²⁷ Thus, there is an unmet need to exploit current computational tools and implement new ones for RNA modeling such as fast screening of small molecules against RNA targets. To this end, Li et al. evaluated two docking programs (GOLD and Glide) and concluded that they are helpful in RNA-based drug discovery.²⁸ DOCK6 with implicit solvent models, i.e., GB/SA and PB/SA models, was used to model RNAs and obtained low root-mean-square deviations (RMSDs).¹⁰ AutoDock4 was also modified to dock RNA targets with flexible grids and achieved some degree of success.^{29,30} The knowledge-based DrugScore^{RNA} was parametrized with 670 RNA–ligand and RNA–protein complexes, but only a fair correlation with the experimental binding affinities was observed for a limited set of 15 RNA–ligand complexes.³¹ RiboDock (currently as rDock) has proved to be successful in several drug design cases.^{12,32,33} The latest version

Received: July 9, 2012

Published: September 4, 2012



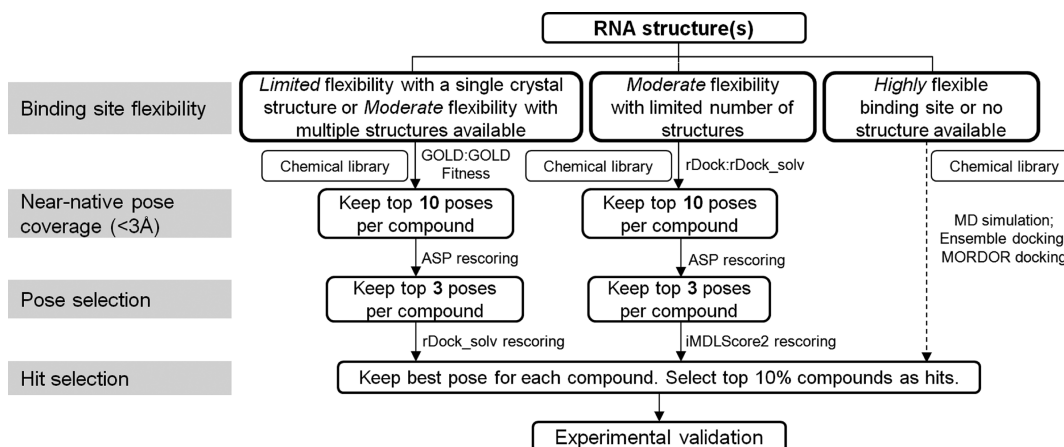


Figure 1. Suggested workflow for structure-based virtual screening for RNA-targeted inhibitor discovery.

of rDock employed a fast weighted solvent accessible surface area (WSAS) to approximate the solvent accessible areas.³² MORDOR (molecular recognition with a driven dynamics optimizer)³⁴ was implemented with induced-fit algorithms for flexible RNA docking. However, as MORDOR is computationally expensive, it is not feasible to screen a large chemical database in an efficient manner. Furthermore, we found that the docking parameters widely used in proteins are not always applicable to RNA systems. For instance, the electrostatic interactions between RNA phosphates and ligands can be overestimated,^{10,27,35} while the desolvation term also needs to be modified.²⁹

To date, due to the challenge of RNA modeling and less developed programs in this field, there have been no reports that provided feasible approaches to address the three critical issues in docking: the accuracy of binding mode prediction, the ranking performance in virtual screening, and accurate scoring.³⁶ Our study aims to identify cost-effective combinations of existing techniques and develop new docking strategies for RNAs. Therefore, we comprehensively evaluated five popular docking programs, including GOLD 5.0.1,³⁷ Glide 5.6,³⁸ Surflex 2.41S,³⁹ AutoDock 4.1,^{40,41} and rDock 2006.2,³² along with 11 scoring functions to explore their capability in RNA docking. On the basis of this study, we proposed a workflow for structure-based modeling for RNA-targeted drug discovery. As illustrated in Figure 1, appropriate docking/scoring combinations need to be used to achieve the best virtual screening performance depending on the flexibility of binding pockets. To maximize the modeling accuracy and improve the enrichment, different modeling strategies can be rationally applied to three critical steps: near-native pose coverage, pose selection, and hit selection. For the first time, intensive statistical analysis was employed in such studies, and we also implemented RNA-specific scoring functions with the largest-ever high-quality RNA–ligand binding affinity data set. Moreover, our study provided new insights into RNA–small molecule interactions, and this helped us explore the best computational strategies for RNA modeling in drug discovery and development.

RESULTS

Reproduction of Experimental Binding Modes. We first examined whether the current protein–ligand derived docking/scoring software could reproduce the ligand binding poses similar to the experimental structures. Ideally, a “good”

RNA docking program should be able to sample all the conformational space and identify at least one near-native pose. Table 1 shows that, if we arbitrarily employed C(5, 3.0 Å) (the top five ranked pose includes at least one near-native pose with RMSD < 3.0 Å) to define a successful docking case, GOLD:GOLD Fitness and rDock:rDock_solv outperformed others, both with a 73.21% success rate. Additionally, GOLD:ChemScore, GOLD:ASP, Glide:GlideScore (SP), Glide:Emodel (SP), and rDock:rDock obtained greater than 50% docking success rates. In contrast, the success rates for Glide:GlideScore (XP), Glide:Emodel (XP), Surflex, and AutoDock4.1 (default) were low, ranging from 30.36 to 44.64%. All programs, especially AutoDock4.1 and Surflex, had weak performances (<60%) on flexible and extensively charged aminoglycosides. When stringent cutoffs such as C(3, 1.5 Å) were used, the accuracy decreased but GOLD:GOLD Fitness and rDock:rDock_solv remained the best (>40%). Results for other programs are available in Table 1.

As expected, we observed that the average docking accuracy for crystal structures was higher than that for NMR structures, for all 11 current docking/scoring combinations (58.84% versus 42.27%, $p = 0.06$). Not surprisingly, the pose reproduction performance on small-molecule RNA ligands was remarkably better than that on flexible aminoglycosides with high statistical significance (64.55% versus 39.51%, $p < 0.01$). Among the failed cases (defined as “two or less docking programs are able to reproduce the near-native structure (RMSD < 3.0 Å) among top five scored poses”), five are crystal structures (2O3V, 2BE0, 2FD0, 2PWT, and 2Z75) and seven are NMR structures (1UUD, 1LVJ, 1TOB, 1AKX, 1EI2, 1KOD, and 1QD3). We found that the current methods were usually less accurate for RNA complexes containing large aminoglycosides (e.g., lividomycin, paromomycin, etc.), weak RNA binders (e.g., arginine and citrulline), or phosphate-containing hydrophilic ligands (glucosamine 6-phosphate). Because the negatively charged moieties can form specific interactions with RNA phosphates in the presence of metal ions acting as the “metal bridge”,⁴² such as 2GDI and 2Z74, we tried docking with consideration of metal ions. As expected, we could significantly improve the pose prediction of the diphosphate tail of thiamine diphosphate in 2GDI when the Mg²⁺ ion was taken into account as part of the RNA targets. When compared with rDock:rDock_solv, the GOLD:GOLD Fitness combination achieved better performance for the pose reproduction on aminoglycoside–RNA complexes such as 1J7T, 2FCZ, 2BE0, 1NEM, and 2TOB,

Table 1. Successful Binding Mode Reproduction of the 56 RNA–Ligand Complexes Using Different Docking/Scoring Combinations with Arbitrary Cutoffs^a

| | GOLD 5.0.1 | | | | AutoDock 4.1 | | | | Surflex 2.415 | | | | Glide 5.6 | | | | rDock 2006.2 | | | | |
|---|---------------|---------------|---------------|-------------------|---------------|--------------------|-----------------|---------------|-----------------|---------------|---------------|--|-----------|---------------|--|-------|--------------|-------|--|-------|--|
| | GOLD Fitness | ChemScore | ASP | Autodock4.1 Score | | Surflex-dock score | GlideScore (SP) | Emodel (SP) | GlideScore (XP) | Emodel (XP) | rDock | | | rDock | | rDock | | rDock | | rDock | |
| aminoglycoside [26] | 18 (9) | 13 (3) | 15 (9) | 1 (1) | | 4 (2) | 12 (3) | 13 (3) | 4 (2) | 4 (2) | 13 (6) | | | 16 (8) | | | | | | | |
| small molecule [30] | 23 (15) | 17 (10) | 22 (15) | 16 (9) | 21 (13) | 18 (13) | 18 (13) | 16 (11) | 15 (11) | 15 (11) | 21 (13) | | | 25 (15) | | | | | | | |
| X-ray crystal [36] | 29 (19) | 26 (13) | 29 (21) | 13 (8) | 17 (11) | 20 (9) | 21 (9) | 12 (8) | 12 (8) | 12 (8) | 24 (16) | | | 29 (17) | | | | | | | |
| NMR [20] | 12 (5) | 4 (0) | 8 (3) | 4 (2) | 8 (4) | 10 (7) | 10 (7) | 8 (5) | 7 (5) | 7 (5) | 10 (3) | | | 12 (6) | | | | | | | |
| total [56] | 41 (24) | 30 (13) | 37 (24) | 17 (10) | 25 (15) | 30 (16) | 31 (16) | 20 (13) | 19 (13) | 19 (13) | 34 (19) | | | 41 (23) | | | | | | | |
| overall success rate, % | 73.21 (42.86) | 53.57 (23.21) | 66.07 (42.86) | 30.36 (17.86) | 44.64 (26.79) | 53.57 (28.57) | 55.36 (28.57) | 35.71 (23.21) | 33.93 (23.21) | 33.93 (23.21) | 60.71 (33.93) | | | 73.21 (41.07) | | | | | | | |
| VUS, ^b % | 78.11 | 65.48 | 70.17 | 43.30 | 55.22 | 65.41 | 66.01 | NA | NA | NA | 63.09 | | | 73.13 | | | | | | | |
| score–binding affinity correln (R^2) ^c | 0.25 | 0.03 | 0.29 | 0.22 | 0.05 | 0.10 | 0.14 | NA | NA | NA | 0.15 | | | | | | | | | | |

^aThe values in the brackets indicate the total number of complexes in that category. The values before the parentheses were results satisfying C(5, 3.0 Å), and the values in the parentheses were derived with the stringent criterion C(3, 1.5 Å) (described in the Materials and Methods). The Glide XP mode could not obtain enough data with the stringent restraints; thus the VUS values and R^2 are not available.
^bVolume under the surface.
^cExcluding 1TOB, 2TOB, and 1LVJ when calculating Pearson correlation coefficients.

whereas rDock:rDock_solv was more accurate for druglike ligands including 2Z74, 2Z75, 1EHT, and 1AKX. The detailed results (scores, RMSDs, and statistics) are available in Tables S3 and S4 in the Supporting Information.

To better demonstrate the relation of the docking accuracy with RMSD and ranking, we illustrated our results with Figure 2A, in which the heavy-atom RMSD and the ranking of pose were considered at the same time. The volume under the surface (VUS) represents the overall capacity of reproducing the near-native binding modes. It shows that GOLD:GOLD Fitness achieved the best VUS (78.11%), while rDock:rDock_solv was the second best (Table 1 and Figure 2A). We proposed to employ the contour of 50% success rate to guide the pose selection in RNA docking: if one aims to cover at least one near-native pose (RMSD < 3.0 Å) in 50% of the ligands, at least the top five poses should be kept when using GOLD:GOLD Fitness. In contrast, we should keep at least the top 20 poses to achieve 50% success for Surflex and AutoDock 4.1 (Figure 2B). From these assessments, we suggest that GOLD:GOLD Fitness and rDock:rDock_solv are the best methods for pose predictions in RNA docking, as proposed in Figure 1.

Rescoring To Improve Near-Native Binding Pose Ranking. To improve the pose ranking accuracy with rescoring, we assessed the scoring function capability of differentiating the ligand crystal/NMR structures from their decoy poses. This was done by investigating two parameters: the ranking of native poses and Spearman's correlation between scores and RMSDs.

Generally, an ideal scoring function should rank the crystal/NMR and very-near-native poses statistically higher than other decoys. Since GOLD:GOLD Fitness outperformed other docking programs on the coverage of the near-native poses as aforementioned, it was utilized to generate 100 decoys for each target with the hope of covering a wide range of poses, from near-native to decoy poses. We investigated whether a given scoring function could obtain the highest rankings for experimentally determined ligand poses. Analogous to IC₅₀ (in assessing biological activity), we used 50% success rate to evaluate the performance of different docking/scoring methods. As demonstrated in Figure 2C, the 50% success rate line (dotted line) clustered these scoring functions into three groups: ASP, ChemScore, AutoDock4.1 Score and Emodel (SP), were the first group; the second group included other scoring functions, except rDock, which ranked the lowest as the third group. Figure 2C indicated that GOLD Fitness has 50% possibility to rank the native ligand conformation within the top 10% of the predicted poses, whereas for ASP, ChemScore, AutoDock4.1 Score, and Emodel (SP) this value was reduced to the top 5%. The native pose ranking performance for different docking/scoring schemes varied with different RNA target structures. For example, most programs performed significantly better for crystal structures than for NMR structures (69.14% versus 38.89%, $p < 0.01$) with the top 10 as the cutoff to define a successful ranking case. Surprisingly, ASP was remarkably better in crystal structure ranking, in which only two targets (2O3V and 3DIL) failed, while AutoDock4.1 outperformed others in ranking NMR structures. Taken together, these data suggested that RNA targets with different structural resolutions should be rescored with respective appropriate scoring functions (e.g., ASP or AutoDock4.1) after the initial step of docking with GOLD:GOLD Fitness or

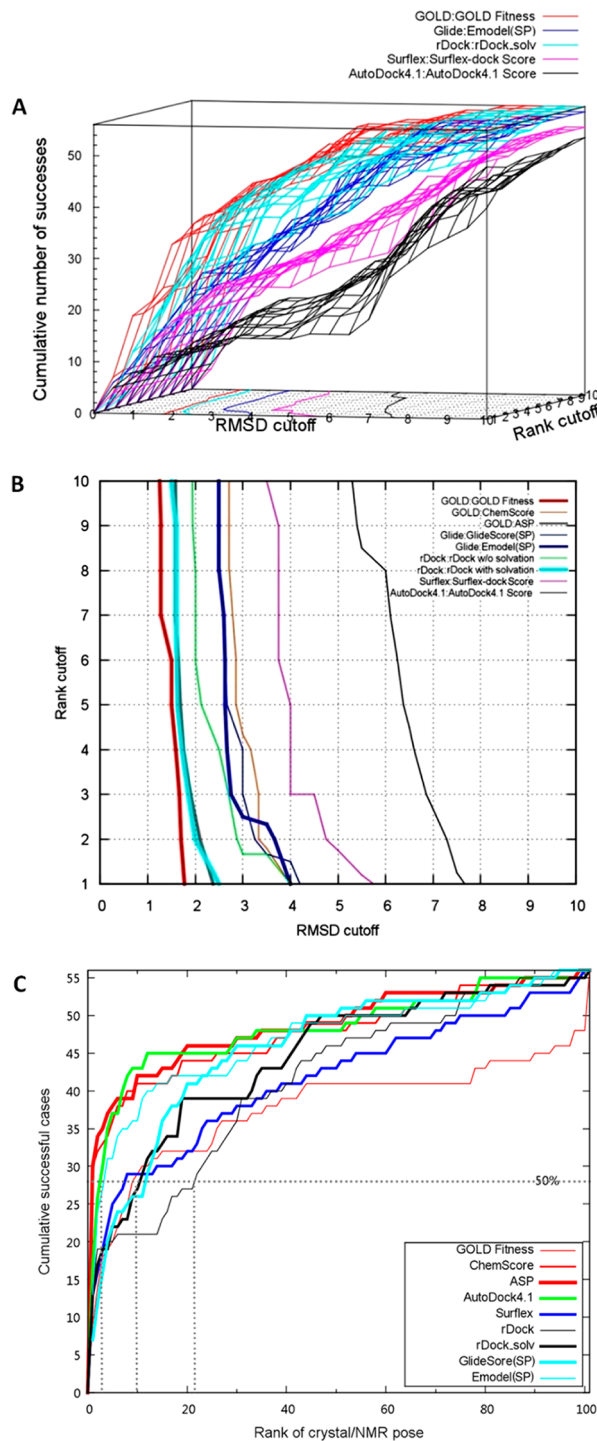


Figure 2. The 3D cumulative success rate from the binding mode reproduction experiments. (A) The cumulative success rate in 3D representation was calculated based on a series of $C(X, Y \text{ \AA})$. Only scoring functions which obtained the highest VUS values for each docking program were selected for illustration. The contour on the XY (RMSD–rank) plane represents the 50% ($Z = 28$) success rate (the binding mode can be reproduced for 50% of RNA–ligand complexes). (B) The 50% success contour ($Z = 28$) for all available scoring functions (GlideScore (XP) and Emodel (XP) were not included due to the unavailability of VUS values). (C) Cumulative success rate for 56 RNA–ligand complexes based on the ranking of X-ray/NMR determined poses against 100 decoys. The 50% success line and the corresponding rankings to achieve 50% success are shown as dotted lines.

rDock:rDock_solv. Detailed results of this ranking study are available in Table S5 in the Supporting Information.

The score–RMSD correlation is another parameter related to the ranking capability. Here we investigated this parameter using Spearman’s rank correlation because it is known that RMSD is not linearly correlated with docking scores.²⁹ Our study showed that in most cases RMSD and docking scores were positively correlated, as desired, but the correlations varied for different RNA targets. Thus, we grouped the 56 RNA targets based on the strength of the correlation for each scoring function (see Materials and Methods). ASP, GlideScore (SP), and Emodel (SP) were the best three scoring functions which had the most cases with a moderate or strong correlation between the RMSD and the score (Table 2). rDock,

Table 2. Score–RMSD Spearman’s Rank Correlations for Various Scoring Functions^a

| | weak | moderate | strong |
|--------------------|------|----------|--------|
| GOLD Fitness | 44 | 5 | 7 |
| ChemScore | 41 | 7 | 8 |
| ASP | 33 | 15 | 8 |
| GlideScore (SP) | 31 | 15 | 10 |
| Emodel (SP) | 29 | 14 | 13 |
| Surflex-dock Score | 38 | 12 | 6 |
| AutoDock4.1 Score | 40 | 5 | 11 |
| rDock | 35 | 12 | 9 |
| rDock_solv | 36 | 12 | 8 |

^aThe values indicate the number of RNA–ligand complexes fit in each correlation category (weak, $\rho < 0.3$; moderate, $0.3 \leq \rho < 0.5$; strong, $\rho \geq 0.5$).

rDock_solv, and Surflex-dock scores obtained fair performances, which could derive weak or strong correlations for more than one-third of the cases. Surprisingly, GOLD Fitness could not achieve satisfactory performance to enrich the near-native ligand conformations (44 cases obtained the weak correlations) (Table 2). Combined with the native pose ranking analysis, these results demonstrated that other scoring functions such as ASP could enrich the near-native poses when applied to decoy poses generated by GOLD:GOLD Fitness.

As we have identified ASP as the best scoring function for ranking RNA ligand poses, we wanted to further study whether it could improve the identification of the near-native binding poses generated by GOLD:GOLD Fitness. Table S4 in the Supporting Information showed that when all top 10 poses generated by GOLD:GOLD fitness were rescored by the ASP scoring function, the number of RNA targets satisfying $C(S, 3.0 \text{ \AA})$ increased from 41 to 44, while this number for $C(3, 1.5 \text{ \AA})$ increased from 24 to 30, compared to the original GOLD:GOLD Fitness performance. Specifically, we observed that the best RMSD in the top 5 scored docking conformations of 2GDI, 2Z74, 2PWT, and 1ZZ5 was significantly reduced (below 3.0 \AA) after ASP rescored (Supplementary Figure 1 and Table S4 in the Supporting Information). In contrast, GOLD:GOLD Fitness alone failed to identify the near-native conformation for these targets. Furthermore, the VUS increased from 78.11 to 79.18%. Compared with the docking accuracy using GOLD:GOLD Fitness alone, the average RMSD for the top-scored conformations was further reduced to $2.61 \pm 0.38 \text{ \AA}$ after ASP rescored (Table S4 in the Supporting Information). Combined with native pose ranking and RMSD–score correlation results, our results confirmed that ASP has the

best ability for pose ranking, and ASP rescoring can significantly enrich the near-native decoys for the purpose of pose reproduction in RNA docking. Thus, ASP rescoring seems to be a reliable method for pose selection in a virtual screening exercise (Figure 1).

Development of New RNA-Specific Scoring Functions for RNA–Ligand Binding Affinity Prediction. As most of the scoring functions used to predict RNA–ligand binding affinity were optimized for protein–ligand interactions, there is a demand for careful evaluation of existing scoring schemes and implementation of new RNA-specific methods. Since the determination of RNA–ligand binding affinities depends on multiple factors (e.g., temperature, assay method), we carefully curated 45 RNA complexes with reported binding affinities (K_d) (Table S2 in the Supporting Information). The score–binding affinity correlations were calculated for the selected scoring functions. As expected, the correlation coefficients (R^2) for all evaluated scoring functions were low ($R^2 < 0.3$). The values are shown in Table 1, and the score–binding affinity plots for the best three scoring functions (ASP, GOLD Fitness, and AutoDock4.1 Score (default)) are available in Supplementary Figure 2 in the Supporting Information.

To improve the result, we developed scoring functions with our large RNA–ligand data set with available binding affinities. This was done by optimizing AutoDock4.1 scoring terms using multilinear regression (MLR) methods. During the implementation, only four terms were optimized because (1) the charge-based desolvation energy function employed by AutoDock4.1 was based on Wesson and Eisenberg's model,⁴³ which was entirely trained by protein targets, and (2) the solvent accessible surface area calculation in this model was simplified by using the interatomic contact radius.⁴¹ Upon MLR optimization, the contributions of those scoring terms are 0.1460 for van der Waals (vdW), 0.0745 for hydrogen bonding (hbond), 0.0559 for electrostatic, and 0.3073 for torsions. This new score function was named "iMDLScore1". Since the training set for iMDLScore1 includes diverse RNA binders, varying from tiny hypoxanthines to large aminoglycosides, we observed a significant contribution of vdW interactions. As illustrated in Figure 3A, we achieved a much better correlation ($R^2 = 0.70$) between docking scores and binding affinities after optimizing the coefficients of AutoDock4.1 scoring terms. When iMDLScore1 was further validated against an external test set consisting of eight complexes, the correlation coefficient between the score and binding affinity was 0.82, and the root-mean-square error (RMSE) of prediction was as low as 4.09 kJ/mol.

A known challenge in RNA virtual screening is how to enrich the active compounds from a focused library with charged molecules because most RNA binders are potentially positively charged.²⁷ To overcome this problem, we derived a second scoring function, iMDLScore2, with a data set containing 18 complexes with positively charged ligands. In iMDLScore2 the contribution of the electrostatic term to the docking scores was over 10%. Interestingly, R^2 and Q^2 (leave-one-out cross-validation R^2) for the training set reached 0.79 and 0.62, respectively (Figure 3B), and R^2 for the test set was 0.76. Additionally, the RMSE of prediction was comparable to that of iMDLScore1 (4.35 kJ/mol). Q^2 , R^2 , and the RMSE of prediction indicated the good predictive capability of RNA–ligand binding affinities by iMDLScore2. The new coefficients in iMDLScore2 were 0.1634 (vdW), 0.2436 (hbond), 0.2311 (electrostatic), and 0.2212 (torsion). Obviously, the contribu-

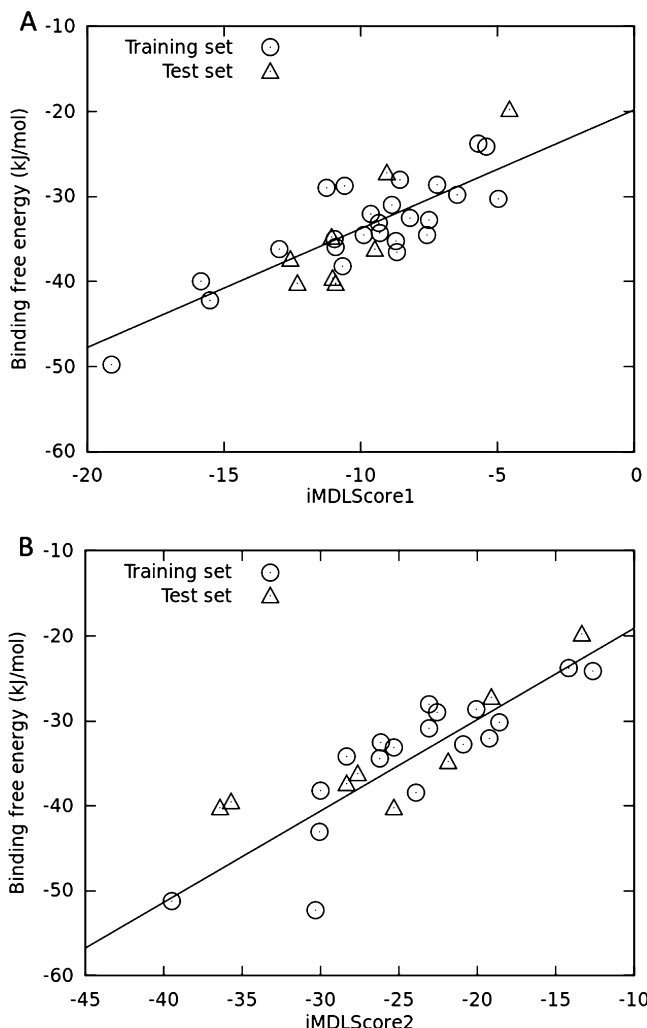


Figure 3. Correlation between docking scores and experimental binding affinity for iMDLScore1 and iMDLScore2.

tions of electrostatic and hbond were increased. This result indicated that polar non-bonded interactions are critical attributes for accurately predicting the relative binding affinity for charged ligands. All results and parameters for the new scoring functions can be found in Table 3. As indicated in Figure 1, we observed the improvement of the virtual screening enrichment for a moderately flexible RNA target by the implementation of our new scoring functions (see below).

Table 3. Contributions of AutoDock4.1 Energetic Terms and Associated R^2 , Q^2 , and RMSE of Prediction

| parameter | default | iMDLScore1 | iMDLScore2 |
|---------------------------------------|---------|------------|------------|
| vdW | 0.1662 | 0.146 | 0.1634 |
| hbond | 0.1209 | 0.07451 | 0.2436 |
| electrostatic | 0.1406 | 0.05593 | 0.2311 |
| desolvation | 0.1322 | 0 | 0 |
| torsion | 0.2983 | 0.3073 | 0.2212 |
| no. of complexes as training set | NA | 25 | 18 |
| R^2 (training set) | 0.22 | 0.70 | 0.79 |
| LOO Q^2 (training set) | NA | 0.44 | 0.62 |
| R^2 (test set) | NA | 0.82 | 0.76 |
| RMSE of prediction (kJ/mol, test set) | NA | 4.09 | 4.35 |

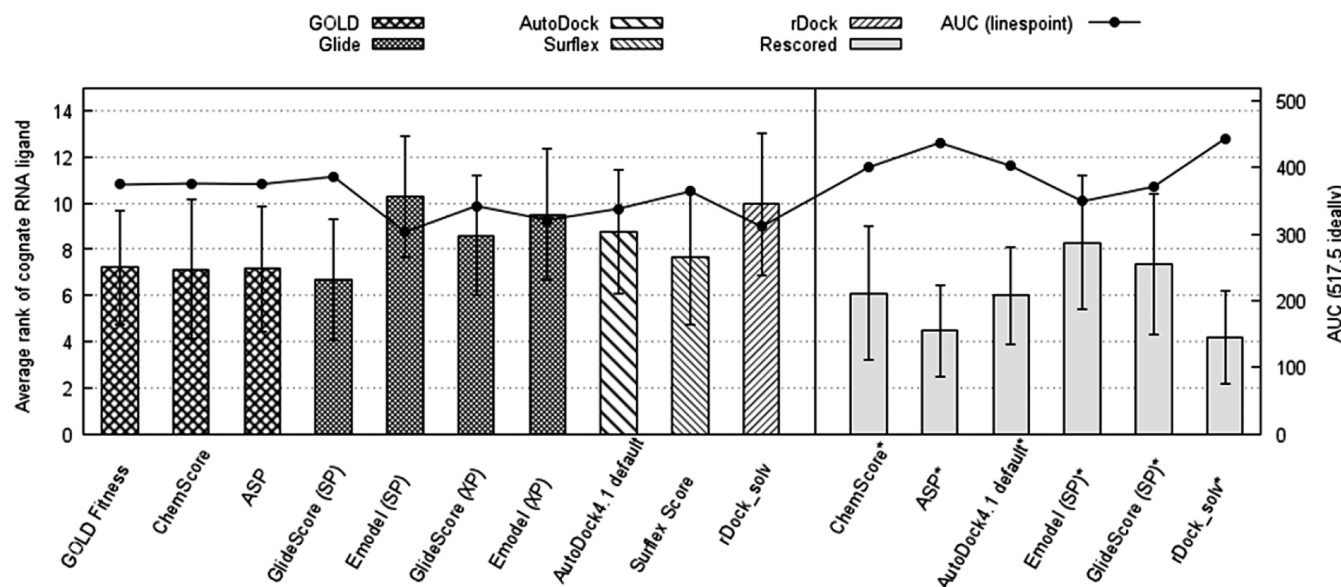


Figure 4. Average ranking of the cognate ligands and AUC in the cross-docking study. The heights of boxes represent the average rankings of the cognate ligands of the 23 RNA targets, while the lines and points are for the AUC. The AUC was calculated from the cumulative number of RNA targets in which the ranking of the cognate ligands was below different cutoffs. The error bars represent the 95% confidence interval from the 23 cross-docking cases. The asterisks (*) represent the method of rescoring based on the top 10 predicted poses by GOLD:GOLD Fitness. Ideally, AUC is 517.5 if all cognate ligands are ranked on the top one.

Identification of Rescoring Scheme To Improve the Cross-Docking Performance. We employed a cross-docking study to explore the best docking/scoring strategy to identify the cognate ligands for their corresponding RNA targets. Among the 56 RNA complexes, we selected a diversity subset of 16 crystal structure and 7 NMR structures for which we obtained good pose reproduction rates. As anticipated, no single docking program could lead to satisfactory enrichment in terms of the average rankings of cognate ligands (e.g., average ranking below 5 out of 23). Glide:GlideScore (SP) achieved the best average ranking of the cognate ligands (6.70 ± 2.63), whereas GOLD-associated scoring functions had similar performances: 7.22 ± 2.45 for GOLD Fitness, 7.13 ± 3.01 for ChemScore, and 7.17 ± 2.71 for ASP (Figure 4). Glide:GlideScore (SP) acquired the best recovery AUC (area under the curve) of cross-docking (74.66%), but the performance of Glide:Emodel (SP) was the least ideal (AUC = 58.61%).

To improve the cross-docking performance, we rescored the top 10 poses generated by GOLD:GOLD Fitness with ChemScore, ASP, AutoDock4.1 Score, Emodel (SP), GlideScore (SP), and rDock_solv, because these scoring functions performed well in ranking poses (Figure 2C). Figure 4 and Table S6 in the Supporting Information demonstrated that rDock_solv rescoring achieved the best average ranking of cognate ligands (4.2 ± 2.0) and recovery AUC (85.69%). It ranked 16 cognate ligands on the top 3. As a comparison, Glide:GlideScore (SP), the best cross-docking program above, could only rank 10 cognate ligands on the top 3. When compared with the initial result from GOLD:GOLD Fitness, rDock_solv rescoring improved the ranking of 17 cognate ligands. The ASP rescoring was the second best (after rDock_solv) with an average ranking of 4.4 ± 1.9 and recovery AUC = 84.53%. It improved the ranking of cognate ligands in 15 cases. Therefore, as expected, we confirmed that rescoring could significantly improve both the average ranking of cognate ligands and the recovery AUC.

When comparing the average rankings for low-resolution structures with high-resolution ones, we could group these scoring functions into two categories: soft-core scoring and hard-core scoring. For instance, we think the AutoDock4.1 scoring function is relatively “soft”, which obtained a better cognate ligand ranking for low-resolution RNA structures that may contain unfavorable structural errors (e.g., clashes).⁴⁴ In contrast, ASP and rDock_solv achieved statistically significantly better performances ($p < 0.05$) on high-resolution crystal structures, indicating that they are hard-core scoring methods capable of penalizing structural defects (Table S6 in the Supporting Information). These characterizations were consistent with the results from our above native pose ranking evaluation, where AutoDock4.1 also achieved better performance for NMR structures while ASP was more accurate for ranking high-resolution crystal structures. Moreover, these findings are critical for the selection of proper scoring functions for RNA virtual screening based on the RNA structural flexibility (see below).

Implementation of a Two-Step Scheme for Virtual Screening. Receptor flexibility remains a challenge in structure-based virtual screening.⁴⁵ This has been partially addressed by applying soft potentials, rotamer libraries, and molecular dynamic simulations during/after docking.⁴⁶ Herein, we aim to identify the most rational combination of docking/scoring/rescoring strategies for RNA virtual screening. We utilized two different RNA targets: the bacterial 16S rRNA A-site and the lysine riboswitch. These represent two typical kinds of RNA targets: the bulge-containing A-form helix and aptamer, respectively.

We quantitatively characterized the flexibility of the 16S rRNA A-site (PDB ID: 1J7T) by comparing the *B*-factors of the active site nucleotides (4 Å around paromomycin) with other non-terminal nucleotides. Supplementary Figure 4A in the Supporting Information showed that the *B*-factors of the active site were statistically higher than those of the other part of the RNA ($p = 0.002$), indicating that the inhibitor binding pocket is

Table 4. ROC AUC for Different Docking and Scoring Function Combinations in RNA Virtual Screening Study

| initial docking and scoring function | rescoring function | bacterial rRNA A-site (1J7T) | | | lysine riboswitch (3DIL) | |
|--------------------------------------|--------------------|------------------------------|----------------------------|-------------------------------|---------------------------------|---------------------------------|
| | | aminoglycosides ^a | Zhou data set ^a | Foloppe data set ^a | 7 known inhibitors ^a | 7 known inhibitors ^b |
| GOLD:GOLD Fitness | none | 1.0 | 1.0 | 0.58 | 0.97 | 0.82 |
| rDock:rDock_solv | none | 1.0 | 1.0 | 0.61 | 0.999 | 0.86 |
| GOLD:GOLD Fitness | ASP | NA | NA | 0.50 | 0.98 | 0.51 |
| GOLD:GOLD Fitness | rDock_solv | NA | NA | 0.68 | 0.998 | 0.86 |
| GOLD:GOLD Fitness | AutoDock4.1 Score | NA | NA | 0.64 | 0.77 | NA |
| GOLD:GOLD Fitness | iMDLScore1 | NA | NA | 0.58 | 0.66 | NA |
| GOLD:GOLD Fitness | iMDLScore2 | NA | NA | 0.69 | 0.92 | 0.51 |
| rDock:rDock_solv | AutoDock4.1 Score | NA | NA | 0.67 | 0.46 | NA |
| rDock:rDock_solv | iMDLScore1 | NA | NA | 0.61 | 0.33 | NA |
| rDock:rDock_solv | iMDLScore2 | NA | NA | 0.74 | 0.81 | 0.51 |

^aThe decoy set was the MayBridge data set. ^bThe decoy set was seven known lysine analogues inactive to the lysine riboswitch.

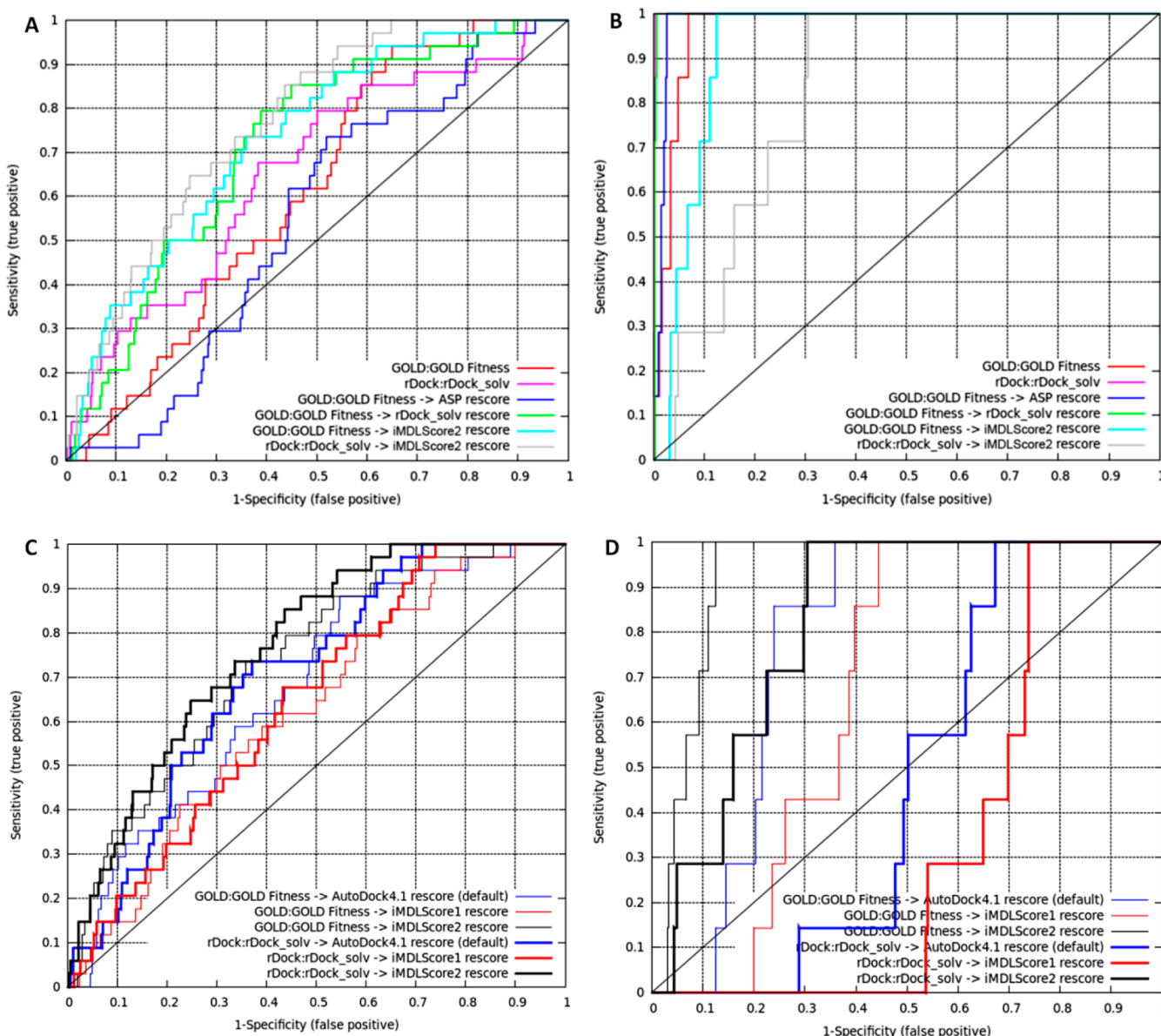


Figure 5. ROC curves of the virtual screening experiments with various docking/scoring combinations. (A) Virtual screening against the 16S rRNA A-site using the Foloppe data set. (B) Virtual screening against the lysine riboswitch using seven known active compounds. (C, D) ROC comparison of the virtual screening performances of AutoDock4.1 and iMDLScore1/iMDLScore2 scoring functions with rRNA A-site (C) and lysine riboswitch (D). GOLD:GOLD Fitness dockings are in thin lines, while rDock:rDock_solv dockings are in thick lines. AutoDock4.1 default scoring function, iMDLScore1, and iMDLScore2 are colored red, blue, and black, respectively.

flexible. Furthermore, normal mode analysis with oGNM⁴⁷ confirmed this local flexibility because significant fluctuations of the binding pocket nucleotides (arrow highlighted) could be observed within the five lowest-frequency modes (low-frequency motions are expected to have larger contributions to the conformational changes⁴⁸). In particular, four critical A-site nucleotides (A16, A17, A38, and A39, equivalent to A1492 and A1493 in the *E. coli* rRNA nucleotide numbering) were predicted to have the largest atomic fluctuations (Supplementary Figure 4B in the Supporting Information). Our analyses agreed with the findings that great conformational changes occur upon paromomycin binding and that A1492 and A1493 nucleosides can fluctuate between the extra- and intrahelical states.^{49,50} Detailed analysis of the binding site flexibility is available in the Supporting Information.

The virtual screening against the 16S rRNA A-site showed that, for 31 aminoglycoside mimetics and 11 aminoglycosides, both GOLD:GOLD Fitness and rDock:rDock_solv achieved extremely excellent virtual screening enrichment against MayBridge druglike decoys (receiver operating characteristic (ROC) AUC = 1.0, Table 4). However, they could not obtain reasonable results for the Foloppe data set.¹² rDock:rDock_solv obtained the best enrichment with only AUC = 0.61, while for GOLD:GOLD Fitness the AUC is 0.58 (Table 4). Therefore, we concentrated on exploring novel strategies to improve the enrichment of virtual screening of druglike, positively charged compounds (Foloppe data set). Surprisingly, GOLD:GOLD Fitness coupled with rDock_solv or ASP rescoring did not improve the results (Figure 5A and Table 4). However, the enrichment was significantly increased by rescoring either rDock:rDock_solv or GOLD:GOLD Fitness generated poses using our new scoring function iMDLScore2 with AUC = 0.74 and 0.69, respectively (Figure 5A and Table 4). The AUC difference between one-step and two-step virtual screening indicated that, if the binding modes are well covered (e.g., by GOLD:GOLD Fitness or rDock:rDock_solv), rescoring (e.g., by iMDLScore2) could significantly affect the enrichment in virtual screening. As demonstrated in Figure 5C and Table 4, we also found that the enrichment of virtual screening against the 16S rRNA A-site was positively correlated with the weight of polar interactions ($W_{\text{elec}} + W_{\text{hbond}}$) when iMDLScore2 was used for rescoring. Therefore, we suggested that a soft-core rescoring function that favors electrostatic and hydrogen bond interactions (e.g., iMDLScore2) may be good for a flexible target such as the rRNA A-site.

In contrast, the results from virtual screening against the rigid and closed lysine riboswitch were different. Based on the crystal structure, the ligand (lysine) is completely enveloped in the rigid binding pocket of the lysine riboswitch, and only the small molecules which can sterically fit the pocket can be accommodated.^{51,52} The B-factor analysis demonstrated that the lysine-binding pocket is not flexible (Supplementary Figure 4A in the Supporting Information). Normal mode analysis further confirmed the rigidity of this pocket as no significant atomic fluctuation of the active site nucleotides (arrow highlighted) could be observed within the five low-frequency normal modes (Supplementary Figure 4C in the Supporting Information). Our virtual screening showed that rDock:rDock_solv and GOLD:GOLD Fitness had comparable enrichments (Figure 5B). GOLD:GOLD Fitness coupled with ASP or rDock_solv rescoring could improve the enrichment. Unfortunately, all AutoDock4.1 related scoring functions (default, iMDLScore1, and iMDLScore2) could not obtain as good

enrichment (AUC < 0.85) as other rescoring schemes (AUC > 0.95). This might be due to the failure of assigning enough penalties to the steric clashes so that the big molecules were docked into the small and closed lysine-binding pocket (Figure 5B). Additionally, we investigated whether any computational strategies could differentiate the seven known lysine riboswitch inhibitors from the seven experimentally validated lysine-analogue decoys (very low chemical diversity compared to the above experiment with MayBridge decoys). On the basis of this data set, we found that GOLD:GOLD Fitness combined with rDock_solv rescoring achieved the best enrichment (AUC = 0.86) and ranked all seven active compounds on the top eight. As expected, iMDLScore2 rescoring achieved low enrichment (AUC = 0.51) (Table 4).

When comparing our iMDLScore1/iMDLScore2 with the original AutoDock4.1 scoring function, we found that rescoring by iMDLScore2, which has the least vdW contribution but the most electrostatic and hbond contributions, attained the best enrichment against the 16S rRNA A-site with AUC = 0.69 (based on GOLD:GOLD Fitness docking) and 0.74 (based on rDock:rDock_solv docking) (Table 4 and Figure 5C). In contrast, the results from iMDLScore1 rescoring were not ideal. We observed a similar trend (iMDLScore2 (black) > AutoDock4.1 default (blue) > iMDLScore1 (red)) with ROC AUC analysis for the lysine riboswitch, as demonstrated in Table 4 and Figure 5D. In summary, we identified the best combinations for RNA virtual screening: rDock:rDock_solv coupled with iMDLScore2 rescoring could be used for flat, open, and flexible binding sites of RNAs, while GOLD:GOLD Fitness combined with rDock_solv rescoring could be appropriate for closed and rigid RNA targets (Figure 1).

Application of Ensemble Docking/Scoring for Structural Flexibility of RNAs. RNAs are flexible and ligand binding can significantly alter the backbone dihedral angles, which may in turn change the sugar puckering, narrow grooves, and introduce kinks or intercalation.⁵³ For example, when different ligands bind to HIV-1 TAR RNA, the sugar puckering of A22 can switch from C3'-endo (1UUD) to O4'-endo (1UUI), while U23 switches from C3'-endo (1UUD) to C1'-endo (1UUI). The technique of ensemble docking has been widely used in the field of proteins to model flexibility with a limited number of discrete conformations.⁵⁴ The ensemble structures can be obtained from different X-ray crystal structures, NMR models, or normal-mode analysis.^{16,55} To investigate whether ensemble docking could also improve the docking/scoring accuracy in the RNA system, we collected five RNA targets and their alternative conformations in Table 5 for native pose ranking and cross-docking experiments. We found that, when RNA flexibility was modeled by structural ensemble, the results of the native pose ranking were significantly improved using rDock_solv scoring functions for 1LVJ, 1AM0, and 2Z74. As aforementioned, without considering RNA flexibility, we could not obtain reasonable results for these three targets in a native pose ranking study. However, with other methods, except ASP, only a slight improvement of ranking (<10) was observed. We found that the dihedral angle ϵ (C4'-C3'-O3'-P_{i+1}) of U23 (critical for inhibitor binding) in 1LVJ was statistically correlated with the native pose rankings from rDock_solv based on Spearman's rank correlation ($p < 0.05$) (Table S8 in the Supporting Information). This was probably because when ϵ increased, the phosphate of C24 had a better orientation to interact with the positively charge amine group of the ligands. Such

Table 5. PDBs Used To Assess the Ensemble Docking^a

| RNA | ligand type | PDB ID |
|---|------------------------------------|--|
| HIV-1 TAR RNA | PMZ (intercalator) | <u>1LVJ</u> (12 conformer models) |
| AMP aptamer | AMP | <u>1AM0</u> (8 conformer models) |
| HIV-1 TAR RNA | P14 (guanidine-containing ligands) | <u>1UUD</u> , <u>1UUI</u> , <u>1AKX</u> |
| Diels–Alder ribozyme | DAI | <u>1YKV</u> , 1YLS, 1YKQ |
| <i>Thermoanaerobacter tengcongensis glmS</i> ribozyme | glucose 6-phosphate | <u>2Z74</u> , 2H07, 2H0Z, 2Z75, 2GCV, 2H0W, 2GCS |

^aPrimary RNA targets, which had been studied in native pose ranking and cross-docking, are underlined. *Apo* structures or the structures containing different ligands with the primary target are given in italics.

interactions were correctly estimated by the rDock_solv scoring functions and thus obtained better rankings. In the cross-docking experiment, when the RNA flexibility was considered, the rankings of cognate ligands were significantly improved using GOLD:GOLD Fitness coupled with rDock_solv rescoring for both 1LVJ and 1UUD. Unfortunately, the ranking got slightly worse for 1LVJ and 1YKV when GOLD:GOLD Fitness coupled with AutoDock4.1 rescoring was used. Detailed comparative data are available in Table S7 in the Supporting Information. Our study implied that the consideration of RNA flexibility by ensemble docking could be beneficial to docking/scoring accuracy with a hard-core scoring function (e.g., rDock_solv) (Figure 1); however, it also depends on the RNA target and the docking/scoring methods used for modeling.

DISCUSSION

RNA represents a type of important targets for therapeutic development. In this study, we identified novel strategies for RNA–ligand modeling and virtual screening through a thorough and comprehensive evaluation with statistical analysis heavily used. We provided novel insights into four aspects associated with in silico structure-based molecular design against RNAs. First, GOLD:GOLD Fitness and rDock:rDock_solv, found as the best pose predictors for RNA targets, were appropriate for the initial binding mode generation. However, in order to accurately identify the cognate ligands for RNA targets or improve the virtual screening enrichment, an extra step of rescoring of the predicted binding modes is necessary. Second, we found that ASP and AutoDock4.1 scoring functions, rather than GOLD Fitness, were able to enrich the native or near-native poses. This was based on the observation that ASP rescoring could significantly improve the docking accuracy using GOLD:GOLD Fitness generated poses. Third, soft-core potentials (e.g., iMDLScore1 and iMDLScore2) and hard-core potentials (rDock_solv and ASP) should be properly employed based on the structural resolution and flexibility of the binding sites of RNA targets. The binding pocket flexibility can be evaluated using molecular dynamics or computationally less intensive methods such as *B*-factor analysis described in this study. Hard-core scoring functions could produce more accurate results for virtual screening using RNA ensemble structures. Finally, implementation of RNA-specific scoring function (e.g., iMDLScore2) improved the virtual screening enrichment as well as the accuracy of RNA–ligand binding affinity prediction. In summary, the suggested workflow for

structure-based modeling for RNA-targeted drug discovery is illustrated in Figure 1.

Consistent with other docking evaluation reports,⁵⁶ we suggest that good performance in binding mode reproduction does not guarantee success in virtual screening for RNA inhibitor identification. Thereby we proposed a two-step docking/scoring strategy for RNA virtual screening. Although some scoring functions, such as iMDLScore2, can be used in the rescoring (the second step scoring), they are not ideal for the initial pose generation (the first step docking/scoring). We found when iMDLScore2 was used for the initial pose generation, positively charged groups, such as guanidium and amine, were biased to form interactions with the RNA phosphate moieties (Supplementary Figure 3 in the Supporting Information). Based on our evaluation, no existing docking program achieved satisfactory performances in both pose prediction and hit identification. Our two-step strategy performed well by separating conformation-wise pose selection and ligand-wise hit selection using different docking and scoring functions during virtual screening.

The false positives in the selected hits are an overall consequence of incorrectly predicted binding modes and scoring inaccuracy. Here we highlighted the importance of sampling enough conformational space for the final rescoring, as illustrated in Figure 2B. However, virtual screening involves not only the coverage of near-native conformations for each ligand, but also the enrichment of the true binders. Accordingly, we observed that retaining too many poses for rescoring might accumulate noises. For example, Figure 6 illustrated the trend

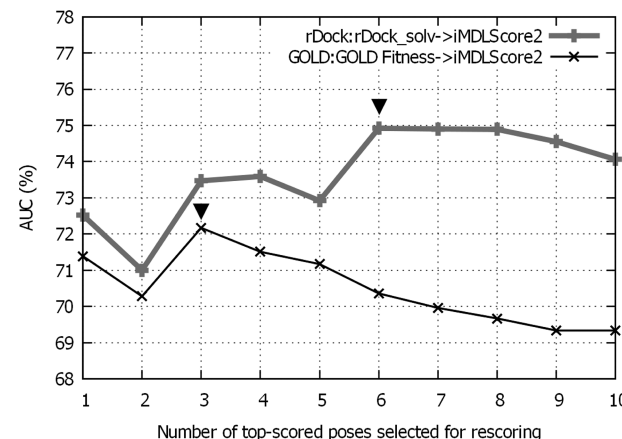


Figure 6. ROC AUC (Y axis) against number of candidate poses (X axis) selected for iMDLScore2 rescoring against 16S rRNA A-site. The downward-pointing triangle (▼) represents the number of picked poses corresponding to the best ROC AUC (turning point).

that only when we picked up the top three poses based on GOLD:GOLD Fitness docking could we achieve the best AUC with iMDLScore2 rescoring. The AUC gradually declined if the number of picked top poses was more than three. A similar trend was also observed for rDock:rDock_solv docking, but the turning point of the number of picked poses was six. We anticipate that, by using GOLD:GOLD Fitness or rDock:rDock_solv as the initial pose generators, retaining top 10 poses for rescoring should be appropriate to cover at least one near-native binding pose without significantly compromising (<3%) the virtual screening enrichment (Figures 2B and 6).

Similar to protein–ligand interactions which are now considered as nonlinear dynamic and cooperative processes,⁴⁶ distal thermodynamic changes may also alter the binding affinity in RNA systems significantly. For example, in the SAM-I riboswitch, the mutations on three base pairs (3GX7) only slightly affect the binding modes, but significantly decrease the binding affinity (~300-fold) (Table S2 in the Supporting Information). Existing scoring functions failed to reflect such a dramatic change in binding affinity quantitatively according to the slight change of the structure. A better estimation of binding affinity via an *in silico* approach may require refinement of the RNA-specific force field, more advanced atom typing, and consideration of structural flexibility. For instance, an RNA-specific WSAS desolvation model was developed instead of inheriting Wesson and Eisenberg's model.^{43,57} In addition, the electrostatic potential in RNAs frequently is not dominated by the negatively charged phosphates because these phosphates can be masked by counterions and waters.²⁷ Therefore, we suggest that advanced scoring functions treat phosphate–ligand and base–ligand interactions differently. In particular, the H-bond formed between RNA bases and aromatic moieties should be considered as more favorable than that formed with phosphate. Rewarding short-range electrostatic and π -related interactions such as aromatic stacking, as rDock does,³² with base atoms could also be beneficial.

Finally, unlike proteins, RNA flexible docking is currently limited by the availability of rotamer libraries of nucleotides. Therefore, RNA flexibility is usually addressed by applying soft grids/potentials,⁵⁸ using ensembles with molecular dynamic simulation or various NMR models,¹⁶ or performing postdocking local optimization.³⁴ Since the force field based optimization algorithms (e.g., MORDOR) are computationally expensive, more studies are needed to reduce the computational cost, probably by either accelerating the force field calculation or alternatively developing novel algorithms for more efficient sampling of ligand-bound conformations. For instance, Rohs et al. utilized Monte Carlo simulation to model flexible DNA–ligand interactions efficiently without any prior binding-site selections,⁵⁹ and this might be applied to RNAs as well. The successful rational design of HIV-1 TAR RNA inhibitors by using structure ensembles from normal-mode analysis represented a good example for the ensemble docking.¹⁶ However, the performance of RNA ensemble docking varies depending on targets, scoring functions, and other factors, in agreement with our assessment here. Sometimes it is possible to cause more noise rather than signals when flexibility is introduced.⁵⁴ Further exploration of RNA flexible docking/scoring will be necessary when more RNA structural data or more RNA flexibility-oriented docking programs become available.

MATERIALS AND METHODS

Data Sets. Most of the currently published data sets are either too small or lack target diversity.^{10,28,29,31,32,34} On the basis of these data sets, we compiled our own data set of high-resolution RNA–ligand complex structures by removing those low-resolution, redundant structures as well as those structures with critical structural defects (e.g., 1AJU). We also included additional structures by mining the Protein Data Bank (PDB) and the literature to identify RNA–ligand complexes with available binding affinities. This resulted in a unique set of 56 RNA–ligand complex structures with 36 high-resolution ($<3.0\text{ \AA}$) crystal and 20 NMR structures. Another issue of the

published data sets was that over 65% of the ligands were aminoglycosides or low-affinity binders (e.g., spermine).²⁸ To avoid the potential problems of statistically overestimating the weight of any typical RNA ligand, we reduced the number of aminoglycosides and low-affinity binders but increased the number of high-affinity small molecules. Our curation encompassed a variety of known RNA targets including RNA aptamers, prokaryotic and eukaryotic rRNA A-sites, ribozymes, riboswitches, and viral RNAs (TAR RNA, HCV IRES domain, etc.). These RNAs are listed in Table S1 in the Supporting Information.

RNA Docking and Decoy Generation. In this article, we have used “A:B” to represent the strategy of “docking using A program and B scoring function”. RNA molecules and ligands were prepared using the Protein Preparation Wizard in Maestro. Briefly, all water molecules, ions, and cofactors were removed. The hydrogen atoms were minimized in the ligand-bound complexes using default parameters. The average structure of NMR models for each complex was minimized and employed for our studies. All of the phosphates in RNAs were deprotonated. The ligands were protonated/deprotonated using Epik (Schrödinger)⁶⁰ at pH 7.0. If an RNA has duplicate binding sites/ligands (e.g., 1J7T), the region with the lowest *B*-factors was used. The ligands were energetically minimized, and molecular docking and rescoring were performed using approaches similar to those previously described.^{28,29,32,61} Briefly, we employed five docking programs (GOLD 5.0.1, Glide 5.6, Surflex v2.415, AutoDock 4.1, and rDock 2006.2) combined with their native scoring functions to generate 10 poses using the default parameters, but with some modifications to ensure the sufficient conformational sampling. In order to ensure the high diversity and quality of the conformational decoys, we employed GOLD:GOLD Fitness to generate 100 conformational decoys for each RNA target with the tuned genetic algorithm parameters. Detailed docking parameters are available in the Supporting Information.

Reproduction of Experimental Structures with Docking. In this study, both RMSDs between experimental structures and predicted docking poses and pose ranking were considered. To simplify the expression, we define $C(X, Y \text{ \AA})$ as the criterion that “at least one near-native binding mode ($<Y \text{ \AA}$ RMSD) was predicted within the top X poses”. To evaluate the overall ability of docking/scoring programs to reproduce experimental structures, we implemented a new parameter, namely, volume under the surface (VUS), to describe the overall performance of binding mode reproduction. As Figure 2A demonstrates, the surface was based on a series of discrete grids. VUS was calculated as the sum of the volumes of all triangular prisms under this surface. Briefly, a series of coordinates were obtained based on their RMSD cutoff (the X dimension), ranking cutoff (the Y dimension), and the number (the Z dimension) of successfully reproduced structures satisfying $C(X, Y \text{ \AA})$. The spacing of RMSD cutoff was 0.5 \AA , and it was 1 for the ranking cutoff. The surface was made by connecting any two adjacent points and then partitioned into a series of triangles. Any of these triangles and their projections on the XY plane was used to define the triangular prism unit. Detailed calculation of the volume of each triangular prism unit and VUS are demonstrated in the Supporting Information. The ideal VUS was calculated as 10 (RMSD cutoff) \times 9 (rank cutoff) \times 56 (number of targets). Different from most of the previous similar studies, if not all, the statistical significance (*p*-value) was always considered for

the analysis throughout this report. Briefly, *p*-values calculated from the Student *t* test were employed to determine the statistical significance when comparing two different groups.

Docked/Native Pose Ranking. For each ligand, we generated 100 decoys to the corresponding RNA target. Therefore, together with the crystal/NMR ligand structure, we obtained 101 RMSD–docking score data points for each cognate RNA–ligand pair. For native pose ranking study, we scored these 101 poses using different docking programs as aforementioned. The rankings of native poses for 56 targets were calculated, and the recovery curves were made as the ranking cutoffs (*X* axis) against the cumulative number of targets (*Y* axis) in which the ranking of the native pose cutoff was smaller than the ranking cutoff. Spearman’s rank correlation coefficient was used to evaluate the ranking capability. To make the docking scores positively correlated with RMSDs (the higher the scores, the higher the RMSD), we used the negative values of GOLD Fitness, ChemScore, ASP, and Surfflex-dock scores. If a pose was assigned a score with an absolute value greater than 1000 (outliers), this RMSD–score pair would be excluded. Spearman’s rank correlation coefficient (ρ) was computed from eq 1:

$$\rho = \frac{\sum_i (r_{\text{RMSD},i} - r_{\text{RMSD}}^{\text{avg}})(r_{\text{score},i} - r_{\text{score}}^{\text{avg}})}{\sqrt{\sum_i (r_{\text{RMSD},i} - r_{\text{RMSD}}^{\text{avg}})^2} \sum_i (r_{\text{score},i} - r_{\text{score}}^{\text{avg}})^2} \quad (1)$$

where $r_{\text{RMSD},i}$ and $r_{\text{score},i}$ are the ranks of the RMSD and score for the pose *i*. We took the average of the ranks for the tied values. $r_{\text{RMSD}}^{\text{avg}}$ and $r_{\text{score}}^{\text{avg}}$ are the average ranks of the RMSD and score for 101 poses. We classified the resulted 56 ρ values (calculated from 56 RNA–ligand complexes) for each scoring function into three groups based on the following widely used criteria: weak correlation, $\rho < 0.3$; moderate correlation, $0.3 \leq \rho < 0.5$; strong correlation, $\rho \geq 0.5$.

Cross-Docking. The data set used for cross-docking was a subset of our overall collection. In order to improve the robustness of cross-docking, we only chose 23 complexes with unique RNAs and a limited number of nonselective ligands (e.g., arginine and aminoglycoside). The RNA–ligand complexes selected for cross-docking are available in Table S6 in the Supporting Information. Cross-docking was performed by docking all 23 ligands in this subset to each RNA target using the methods described in RNA Docking and Decoy Generation. Rescoring was performed based on the top 10 scored poses for each docking method. Cross-docking performance was evaluated by the average ranking of cognate ligand calculated from these 23 RNA targets and the AUC of the recovery curve based on the average ranking of cognate ligands (similar to the recovery curve used in the section Docked/Native Pose Ranking).

Virtual Screening for RNA Inhibitor Identification. Two different targets were assessed, namely, the bacterial 16S rRNA A-site (representing open and flexible binding site) and the lysine riboswitch (representing closed and rigid binding site). The bacterial 16S rRNA A-site and lysine riboswitch structures were obtained from PDB as 1J7T and 3DIL, respectively. We collected 75 known rRNA inhibitors including 34 druglike small molecules from the Foloppe data set¹² and 31 aminoglycoside mimetics from the Zhou data set.¹³ Additionally, we obtained 11 aminoglycoside inhibitors which have crystal structures in complex with the bacterial rRNA A-site (1J7T, 1YRJ, 2F4T, 2ET8, 1LC4, 1MWL, 2BE0, 2G5Q, 2ESI, 2PWT, and 1BYJ). For virtual screening against the lysine

riboswitch, we collected 14 compounds including seven known inhibitors and seven experimentally validated inactives.¹⁷ In order to avoid artificial enrichment,⁶² a focused library containing 942 druglike and positively charged decoys was generated from the MayBridge database. We assumed this randomly constructed decoy library does not include, or includes very few, active compounds as previous studies did.²⁸ The receiver operating characteristic (ROC) curve along with the area under the curve (AUC) was used to assess the overall performance (e.g., recovery rate, enrichment, etc.) of our protocols.

Docking Score–Binding Affinity Correlation. Although it is known that current docking scores are usually poorly correlated with experimental binding affinity,⁵⁶ we are still interested in evaluating the performance of our protocols on RNA targets and trying to learn how to improve the scoring. To this end, dissociation constant (K_d) values were carefully collected from the literature (values and references are available in Table S2 in the Supporting Information), and we compared them with the PDDBind database (<http://www.pdbbind-cn.org/>) and other reports/databases to ensure the consistency of data. If the collected K_d values for each RNA–ligand pair were within a 10-fold difference, the average values were used. Of note, we used 2 μM as the K_d of gentamicin C1a–rRNA A-site complex (1BYJ) for studies because this is the K_d under room temperature, instead of 0.01 μM (K_d under 4 °C).⁶³ Additionally, K_d for neomycin B–HIV-1 TAR RNA complex (1QD3) should be $5.9 \pm 4 \mu\text{M}$. The K_d values used in some previous studies were actually from the U24C mutant.^{29,32,64} The binding free energy was calculated as $\Delta G = RT \ln(K_d)$ under 300 K. The Pearson correlation coefficients (R^2) between these docking scores and their corresponding binding affinities were obtained. Three common outliers, 1LVJ, 1TOB, and 2TOB, were excluded to avoid noise, as they contained many unfavorable steric clashes.

RNA-Specific Scoring Function Optimization. The weak correlation between docking scores and binding affinity might be because most of the current scoring functions were derived from protein–ligand interactions. To implement new RNA-specific scoring functions, we optimized the energetic coefficients in AutoDock4.1 scoring function using our largest-ever RNA–ligand data set with known experimental binding affinities. This empirical scoring function is shown as eq 2.⁴¹

$$\begin{aligned} \Delta G_{\text{bind}} = & W_{\text{vdW}} \sum_{i,j} \left(\frac{A_{ij}}{r_{ij}^{12}} - \frac{B_{ij}}{r_{ij}^6} \right) + W_{\text{hbond}} \\ & \sum_{i,j} \xi(t) \left(\frac{C_{ij}}{r_{ij}^{12}} - \frac{D_{ij}}{r_{ij}^{10}} \right) + W_{\text{elec}} \sum_{i,j} \frac{q_i q_j}{\epsilon(r_{ij}) r_{ij}} \\ & + W_{\text{sol}} \sum_{i,j} (S_i V_j + S_j V_i) e^{-r_{ij}^2/2\sigma^2} + W_{\text{tors}} N_{\text{tors}} \end{aligned} \quad (2)$$

The parameters (A , B , C , D , S , V) were obtained from the default AutoDock4 scoring function, as previously described.⁴¹ With our RNA–ligand data set, we derived a new set of coefficients of five terms (W_{vdW} , W_{hbond} , W_{elec} , W_{sol} , and W_{tors}) with multiple linear regression methods. Besides R^2 , we calculated leave-one-out (LOO) cross-validation correlation coefficients (Q^2) and validated against an external test set consisting of eight complexes to evaluate the predictive power of our new schemes. The PDBs employed to train and validate

iMDLScore1 and iMDLScore2 are listed in Table S2 in the Supporting Information.

■ ASSOCIATED CONTENT

S Supporting Information

Supporting Information methods are the details of docking parameters, VUS calculation, and binding site flexibility analysis. Tables S1–S8 are the PDB codes, RNA–ligand binding affinity data, and the detailed data for binding mode reproduction, native pose ranking, cross-docking, and RNA ensemble docking. Supplementary Figures 1–4 are the pose comparisons, score–binding affinity plots, and binding site flexibility analysis. This material is available free of charge via the Internet at <http://pubs.acs.org>.

■ AUTHOR INFORMATION

Corresponding Author

*Tel.: (713) 745-2958. Fax: (713) 794-5577. E-mail: shuzhang@mdanderson.org

Notes

The authors declare no competing financial interest.

■ ACKNOWLEDGMENTS

Special thanks to Dr. John Liebeschuetz from CCDC for helpful discussions on RNA docking with GOLD. We are also thankful for the free academic licenses from the rDock and AutoDock development teams, and we thank Ms. Xiaofei Xiong for helping in curation of RNA–ligand complexes. This work was partially supported by the U.S. Department of Defense Concept Awards (BC085871), the University Cancer Foundation via the Institutional Research Grant program at the University of Texas M.D. Anderson Cancer Center, M.D. Anderson Prostate SPORE Career Award (P50 CA140388 SPORE), and Grant IRG-08-061-01 from the American Cancer Society. G.A.C. is the Alan M. Gewirtz Leukemia & Lymphoma Society Scholar, and he is supported in part by the CLL Global Research Foundation.

■ REFERENCES

- (1) Bannwarth, S.; Gatignol, A. HIV-1 TAR RNA: the target of molecular interactions between the virus and its host. *Curr. HIV Res.* **2005**, *3*, 61–71.
- (2) Hermann, T. Aminoglycoside antibiotics: old drugs and new therapeutic approaches. *Cell. Mol. Life Sci.* **2007**, *64*, 1841–52.
- (3) Shay, J. W.; Wright, W. E. Telomerase therapeutics for cancer: challenges and new directions. *Nat. Rev. Drug Discovery* **2006**, *5*, 577–84.
- (4) Nicoloso, M. S.; Spizzo, R.; Shimizu, M.; Rossi, S.; Calin, G. A. MicroRNAs—the micro steering wheel of tumour metastases. *Nat. Rev. Cancer* **2009**, *9*, 293–302.
- (5) Thomas, J. R.; Hergenrother, P. J. Targeting RNA with small molecules. *Chem. Rev.* **2008**, *108*, 1171–224.
- (6) Spizzo, R.; Nicoloso, M. S.; Croce, C. M.; Calin, G. A. SnapShot: MicroRNAs in Cancer. *Cell* **2009**, *137*, 586–586 e1.
- (7) Fabbri, M.; Bottone, A.; Shimizu, M.; Spizzo, R.; Nicoloso, M. S.; Rossi, S.; Barbarotto, E.; Cimmino, A.; Adair, B.; Wojcik, S. E.; Valeri, N.; Calore, F.; Sampath, D.; Fanini, F.; Vannini, I.; Musuraca, G.; Dell'Aquila, M.; Alder, H.; Davuluri, R. V.; Rassenti, L. Z.; Negrini, M.; Nakamura, T.; Amadori, D.; Kay, N. E.; Rai, K. R.; Keating, M. J.; Kipps, T. J.; Calin, G. A.; Croce, C. M. Association of a microRNA/TP53 feedback circuitry with pathogenesis and outcome of B-cell chronic lymphocytic leukemia. *JAMA, J. Am. Med. Assoc.* **2011**, *305*, 59–67.
- (8) Melo, S.; Villanueva, A.; Moutinho, C.; Davalos, V.; Spizzo, R.; Ivan, C.; Rossi, S.; Setien, F.; Casanovas, O.; Simo-Riudalbas, L.; Carmona, J.; Carrere, J.; Vidal, A.; Aytes, A.; Puertas, S.; Ropero, S.; Kalluri, R.; Croce, C. M.; Calin, G. A.; Esteller, M. Small molecule enoxacin is a cancer-specific growth inhibitor that acts by enhancing TAR RNA-binding protein 2-mediated microRNA processing. *Proc. Natl. Acad. Sci. U.S.A.* **2011**, *108*, 4394–9.
- (9) Zhang, S.; Chen, L.; Jung, E. J.; Calin, G. A. Targeting microRNAs with small molecules: from dream to reality. *Clin. Pharmacol. Ther.* **2010**, *87*, 754–8.
- (10) Lang, P. T.; Brozell, S. R.; Mukherjee, S.; Pettersen, E. F.; Meng, E. C.; Thomas, V.; Rizzo, R. C.; Case, D. A.; James, T. L.; Kuntz, I. D. DOCK 6: combining techniques to model RNA-small molecule complexes. *RNA* **2009**, *15*, 1219–30.
- (11) Chen, Q.; Shafer, R. H.; Kuntz, I. D. Structure-based discovery of ligands targeted to the RNA double helix. *Biochemistry* **1997**, *36*, 11402–7.
- (12) Foloppe, N.; Chen, I. J.; Davis, B.; Hold, A.; Morley, D.; Howes, R. A structure-based strategy to identify new molecular scaffolds targeting the bacterial ribosomal A-site. *Bioorg. Med. Chem.* **2004**, *12*, 935–47.
- (13) Zhou, Y.; Gregor, V. E.; Ayida, B. K.; Winters, G. C.; Sun, Z.; Murphy, D.; Haley, G.; Bailey, D.; Froelich, J. M.; Fish, S.; Webber, S. E.; Hermann, T.; Wall, D. Synthesis and SAR of 3,5-diaminopiperidine derivatives: novel antibacterial translation inhibitors as aminoglycoside mimetics. *Bioorg. Med. Chem. Lett.* **2007**, *17*, 1206–10.
- (14) Du, Z.; Lind, K. E.; James, T. L. Structure of TAR RNA complexed with a Tat-TAR interaction nanomolar inhibitor that was identified by computational screening. *Chem. Biol.* **2002**, *9*, 707–12.
- (15) Filikov, A. V.; Mohan, V.; Vickers, T. A.; Griffey, R. H.; Cook, P. D.; Abagyan, R. A.; James, T. L. Identification of ligands for RNA targets via structure-based virtual screening: HIV-1 TAR. *J. Comput.-Aided Mol. Des.* **2000**, *14*, 593–610.
- (16) Stelzer, A. C.; Frank, A. T.; Kratz, J. D.; Swanson, M. D.; Gonzalez-Hernandez, M. J.; Lee, J.; Andricioaei, I.; Markovitz, D. M.; Al-Hashimi, H. M. Discovery of selective bioactive small molecules by targeting an RNA dynamic ensemble. *Nat. Chem. Biol.* **2011**, *7*, 553–9.
- (17) Blount, K. F.; Wang, J. X.; Lim, J.; Sudarsan, N.; Breaker, R. R. Antibacterial lysine analogs that target lysine riboswitches. *Nat. Chem. Biol.* **2007**, *3*, 44–9.
- (18) Daldrop, P.; Reyes, F. E.; Robinson, D. A.; Hammond, C. M.; Lilley, D. M.; Batey, R. T.; Brenk, R. Novel ligands for a purine riboswitch discovered by RNA-ligand docking. *Chem. Biol.* **2011**, *18*, 324–35.
- (19) Mulhbacher, J.; Brouillette, E.; Allard, M.; Fortier, L. C.; Malouin, F.; Lafontaine, D. A. Novel riboswitch ligand analogs as selective inhibitors of guanine-related metabolic pathways. *PLoS Pathog.* **2010**, *6*, e1000865.
- (20) Pushechnikov, A.; Lee, M. M.; Childs-Disney, J. L.; Sobczak, K.; French, J. M.; Thornton, C. A.; Disney, M. D. Rational design of ligands targeting triplet repeating transcripts that cause RNA dominant disease: application to myotonic muscular dystrophy type 1 and spinocerebellar ataxia type 3. *J. Am. Chem. Soc.* **2009**, *131*, 9767–79.
- (21) Arambula, J. F.; Ramisetty, S. R.; Baranger, A. M.; Zimmerman, S. C. A simple ligand that selectively targets CUG trinucleotide repeats and inhibits MBNL protein binding. *Proc. Natl. Acad. Sci. U.S.A.* **2009**, *106*, 16068–73.
- (22) Wong, C. H.; Fu, Y.; Ramisetty, S. R.; Baranger, A. M.; Zimmerman, S. C. Selective inhibition of MBNL1-CCUG interaction by small molecules toward potential therapeutic agents for myotonic dystrophy type 2 (DM2). *Nucleic Acids Res.* **2011**, *39*, 8881–90.
- (23) Young, D. D.; Connelly, C. M.; Grohmann, C.; Deiters, A. Small molecule modifiers of microRNA miR-122 function for the treatment of hepatitis C virus infection and hepatocellular carcinoma. *J. Am. Chem. Soc.* **2010**, *132*, 7976–81.
- (24) Gumireddy, K.; Young, D. D.; Xiong, X.; Hogenesch, J. B.; Huang, Q.; Deiters, A. Small-molecule inhibitors of microRNA miR-21 function. *Angew. Chem., Int. Ed.* **2008**, *47*, 7482–4.
- (25) Parsons, J.; Castaldi, M. P.; Dutta, S.; Dibrov, S. M.; Wyles, D. L.; Hermann, T. Conformational inhibition of the hepatitis C virus internal ribosome entry site RNA. *Nat. Chem. Biol.* **2009**, *5*, 823–5.

- (26) Seth, P. P.; Miyaji, A.; Jefferson, E. A.; Sannes-Lowery, K. A.; Osgood, S. A.; Propst, S. S.; Ranken, R.; Massire, C.; Sampath, R.; Ecker, D. J.; Swayze, E. E.; Griffey, R. H. SAR by MS: discovery of a new class of RNA-binding small molecules for the hepatitis C virus: internal ribosome entry site IIA subdomain. *J. Med. Chem.* **2005**, *48*, 7099–102.
- (27) Foloppe, N.; Matassova, N.; Aboul-Ela, F. Towards the discovery of drug-like RNA ligands? *Drug Discovery Today* **2006**, *11*, 1019–27.
- (28) Li, Y.; Shen, J.; Sun, X.; Li, W.; Liu, G.; Tang, Y. Accuracy assessment of protein-based docking programs against RNA targets. *J. Chem. Inf. Model.* **2010**, *50*, 1134–46.
- (29) Detering, C.; Varani, G. Validation of automated docking programs for docking and database screening against RNA drug targets. *J. Med. Chem.* **2004**, *47*, 4188–201.
- (30) Moitessier, N.; Westhof, E.; Hanessian, S. Docking of aminoglycosides to hydrated and flexible RNA. *J. Med. Chem.* **2006**, *49*, 1023–33.
- (31) Pfeffer, P.; Gohlke, H. DrugScoreRNA—knowledge-based scoring function to predict RNA-ligand interactions. *J. Chem. Inf. Model.* **2007**, *47*, 1868–76.
- (32) Morley, S. D.; Afshar, M. Validation of an empirical RNA-ligand scoring function for fast flexible docking using Ribodock. *J. Comput.-Aided Mol. Des.* **2004**, *18*, 189–208.
- (33) Pinto, I. G.; Guilbert, C.; Ulyanov, N. B.; Stearns, J.; James, T. L. Discovery of ligands for a novel target, the human telomerase RNA, based on flexible-target virtual screening and NMR. *J. Med. Chem.* **2008**, *51*, 7205–15.
- (34) Guilbert, C.; James, T. L. Docking to RNA via root-mean-square-deviation-driven energy minimization with flexible ligands and flexible targets. *J. Chem. Inf. Model.* **2008**, *48*, 1257–68.
- (35) Lind, K. E.; Du, Z.; Fujinaga, K.; Peterlin, B. M.; James, T. L. Structure-based computational database screening, in vitro assay, and NMR assessment of compounds that target TAR RNA. *Chem. Biol.* **2002**, *9*, 185–93.
- (36) Kirchmair, J.; Markt, P.; Distinto, S.; Wolber, G.; Langer, T. Evaluation of the performance of 3D virtual screening protocols: RMSD comparisons, enrichment assessments, and decoy selection—what can we learn from earlier mistakes? *J. Comput.-Aided Mol. Des.* **2008**, *22*, 213–28.
- (37) Verdonk, M. L.; Cole, J. C.; Hartshorn, M. J.; Murray, C. W.; Taylor, R. D. Improved protein–ligand docking using GOLD. *Proteins: Struct., Funct., Bioinf.* **2003**, *52*, 609–623.
- (38) Friesner, R. A.; Banks, J. L.; Murphy, R. B.; Halgren, T. A.; Klicic, J. J.; Mainz, D. T.; Repasky, M. P.; Knoll, E. H.; Shelley, M.; Perry, J. K.; Shaw, D. E.; Francis, P.; Shenkin, P. S. Glide: a new approach for rapid, accurate docking and scoring. 1. Method and assessment of docking accuracy. *J. Med. Chem.* **2004**, *47*, 1739–49.
- (39) Jain, A. N. Surflex-Dock 2.1: robust performance from ligand energetic modeling, ring flexibility, and knowledge-based search. *J. Comput.-Aided Mol. Des.* **2007**, *21*, 281–306.
- (40) Morris, G. M.; Goodsell, D. S.; Halliday, R. S.; Huey, R.; Hart, W. E.; Belew, R. K.; Olson, A. J. Automated docking using a Lamarckian genetic algorithm and an empirical binding free energy function. *J. Comput. Chem.* **1998**, *19*, 1639–62.
- (41) Huey, R.; Morris, G. M.; Olson, A. J.; Goodsell, D. S. A semiempirical free energy force field with charge-based desolvation. *J. Comput. Chem.* **2007**, *28*, 1145–52.
- (42) Mayaan, E.; Range, K.; York, D. M. Structure and binding of Mg(II) ions and di-metal bridge complexes with biological phosphates and phosphoranes. *J. Biol. Inorg. Chem.* **2004**, *9*, 807–17.
- (43) Wesson, L.; Eisenberg, D. Atomic solvation parameters applied to molecular dynamics of proteins in solution. *Protein Sci.* **1992**, *1*, 227–35.
- (44) Bindewald, E.; Skolnick, J. A scoring function for docking ligands to low-resolution protein structures. *J. Comput. Chem.* **2005**, *26*, 374–83.
- (45) Rabal, O.; Schneider, G.; Borrell, J. I.; Teixido, J. Structure-based virtual screening of FGFR inhibitors: cross-decoys and induced-fit effect. *BioDrugs* **2007**, *21*, 31–45.
- (46) Chen, L.; Morrow, J. K.; Tran, H. T.; Phatak, S. S.; Du-Cuny, L.; Zhang, S. From Laptop to Benchtop to Bedside: Structure-based Drug Design on Protein Targets. *Curr. Pharm. Des.* **2012**, *18*, 1217–39.
- (47) Yang, L. W.; Rader, A. J.; Liu, X.; Jursa, C. J.; Chen, S. C.; Karimi, H. A.; Bahar, I. oGNM: online computation of structural dynamics using the Gaussian Network Model. *Nucleic Acids Res.* **2006**, *34*, W24–31.
- (48) Dobbins, S. E.; Lesk, V. I.; Sternberg, M. J. Insights into protein flexibility: The relationship between normal modes and conformational change upon protein-protein docking. *Proc. Natl. Acad. Sci. U.S.A.* **2008**, *105*, 10390–5.
- (49) Romanowska, J.; McCammon, J. A.; Trylska, J. Understanding the origins of bacterial resistance to aminoglycosides through molecular dynamics mutational study of the ribosomal A-site. *PLoS Comput. Biol.* **2011**, *7*, e1002099.
- (50) Romanowska, J.; Setny, P.; Trylska, J. Molecular dynamics study of the ribosomal A-site. *J. Phys. Chem. B* **2008**, *112*, 15227–43.
- (51) Garst, A. D.; Heroux, A.; Rambo, R. P.; Batey, R. T. Crystal structure of the lysine riboswitch regulatory mRNA element. *J. Biol. Chem.* **2008**, *283*, 22347–51.
- (52) Serganov, A.; Huang, L.; Patel, D. J. Structural insights into amino acid binding and gene control by a lysine riboswitch. *Nature* **2008**, *455*, 1263–7.
- (53) Patel, D. J.; Suri, A. K.; Jiang, F.; Jiang, L.; Fan, P.; Kumar, R. A.; Nonin, S. Structure, recognition and adaptive binding in RNA aptamer complexes. *J. Mol. Biol.* **1997**, *272*, 645–64.
- (54) Korb, O.; Olsson, T. S.; Bowden, S. J.; Hall, R. J.; Verdonk, M. L.; Liebeschuetz, J. W.; Cole, J. C. Potential and limitations of ensemble docking. *J. Chem. Inf. Model.* **2012**, *52*, 1262–74.
- (55) Tran, H. T.; Zhang, S. Accurate Prediction of the Bound Form of the Akt Pleckstrin Homology Domain Using Normal Mode Analysis To Explore Structural Flexibility. *J. Chem. Inf. Model.* **2012**, *51*, 2352–60.
- (56) Warren, G. L.; Andrews, C. W.; Capelli, A. M.; Clarke, B.; LaLonde, J.; Lambert, M. H.; Lindvall, M.; Nevins, N.; Semus, S. F.; Senger, S.; Tedesco, G.; Wall, I. D.; Woolven, J. M.; Peishoff, C. E.; Head, M. S. A critical assessment of docking programs and scoring functions. *J. Med. Chem.* **2006**, *49*, 5912–31.
- (57) Wang, J.; Wang, W.; Huo, S.; Lee, M.; Kollman, P. A. Solvation Model Based on Weighted Solvent Accessible Surface Area. *J. Phys. Chem. B* **2001**, *105*, 5055–67.
- (58) Kruijger, D. M.; Bergs, J.; Kazemi, S.; Gohlke, H. Target Flexibility in RNA–Ligand Docking Modeled by Elastic Potential Grids. *ACS Med. Chem. Lett.* **2011**, *2*, 489–493.
- (59) Rohs, R.; Bloch, I.; Sklenar, H.; Shakhed, Z. Molecular flexibility in ab initio drug docking to DNA: binding-site and binding-mode transitions in all-atom Monte Carlo simulations. *Nucleic Acids Res.* **2005**, *33*, 7048–57.
- (60) Shelley, J. C.; Cholleti, A.; Frye, L. L.; Greenwood, J. R.; Timlin, M. R.; Uchimaya, M. Epik: a software program for pK(a) prediction and protonation state generation for drug-like molecules. *J. Comput.-Aided Mol. Des.* **2007**, *21*, 681–91.
- (61) Holt, P. A.; Chaires, J. B.; Trent, J. O. Molecular Docking of Intercalators and Groove-Binders to Nucleic Acids Using Autodock and Surflex. *J. Chem. Inf. Model.* **2008**, *48*, 1602–15.
- (62) Verdonk, M. L.; Berdini, V.; Hartshorn, M. J.; Mooij, W. T.; Murray, C. W.; Taylor, R. D.; Watson, P. Virtual screening using protein-ligand docking: avoiding artificial enrichment. *J. Chem. Inf. Comput. Sci.* **2004**, *44*, 793–806.
- (63) Yoshizawa, S.; Fourmy, D.; Puglisi, J. D. Structural origins of gentamicin antibiotic action. *EMBO J.* **1998**, *17*, 6437–48.
- (64) Barbault, F.; Zhang, L.; Zhang, L.; Fan, B. T. Parametrization of a specific free energy function for automated docking against RNA targets using neural networks. *Chemom. Intell. Lab. Syst.* **2006**, *82*, 269–75.